Nuclear Instruments and Methods , A354,547,(1995)

The GILDA mission: a new technique for a gamma-ray telescope in the energy range 20 MeV - 100 GeV

G. Barbiellini[1], M. Boezio[1], M. Casolino[2], M. Candusso[2], M. P. De Pascale[2], A. Morselli[2], P. Picozza[2], M. Ricci[4], R. Sparvoli[2], P. Spillantini[3], A. Vacchi[1]

1 Dept. of Physics, Univ. of Trieste and INFN, Italy
2 Dept. of Physics, II Univ. of Rome "Tor Vergata" and INFN, Italy
3 Dept. of Physics, Univ. of Firenze and INFN, Italy
4 INFN Laboratori Nazionali di Frascati, Italy

1. Introduction

The high energy gamma-ray astrophysics has greatly developed in these last few years because of the results of the experiment EGRET[1], on the Compton Gamma Ray Observatory. The satellite observations have brought more detailed data about the well known gamma-ray sources, but also the discovery of new ones, both galactic and extragalactic, especially Active Galactic Nuclei and gamma-ray bursts. Nevertheless, the emission mechanisms of these sources are still not clear, so it is of crucial importance the investigation of the high energy component of the cosmic gamma radiation with a telescope working in a energy interval broader than EGRET.

The most serious problem affecting the EGRET telescope is the decrease of the detection efficiency at high energies, due to the use of anticoincidence counters placed around the detector. Since at energies greater than 1 GeV the number of secondaries produced in an electromagnetic shower is relevant (more than 100), the probability of having a back scattered particle on the anticoincidence counters, inhibiting in this way the acquisition trigger, becomes quite high, reaching the value of 70% for a 30 GeV gamma.

Another drawback of the EGRET instrument is provided by the spark chambers. They need periodic substitution of the filling gas to work and this requirement brings weight and duration time problems for a space experiment. Moreover, they have quite a long dead time, especially related to the typical length of transient phenomena like the gamma ray bursts. Finally, the track resolution of such detectors is not better than few millimeters. All these problems can be overcome with the adoption of silicon strips detectors.

2. The GILDA apparatus

The core of the GILDA telescope is a modified space version of the silicon calorimeter presently used in the Wizard balloon flights program, to be installed on a future version of the Resource-01 satellite, scheduled to fly at the beginning of the next millennium. This detector is a fine-grained imaging electromagnetic calorimeter conceived for the Wizard experiment to investigate, in a planned space mission, the antimatter component of the primary cosmic radiation [2].

Detectors based on the silicon technology have many advantages for space applications: no gas refilling system or high voltages, no need of photomultipliers (low consumption), short dead time, possibility of self triggering. During the project phase, the calorimeter has been extensively studied with Monte Carlo simulations, and a prototype, containing 20 XY samplings of silicon wafers with strips 3.6 mm wide interleaved with 19 showering tungsten planes (for a total of 9.5 X_0), has already been built and tested at the CERN Proton Synchrotron (PS) [3]. Five planes (50×50 cm^2) have already flown in a

balloon experiment from the NASA base at Fort Sumner (New Mexico) in September 1993; another Si-W calorimeter with 8 planes is ready for a second flight in Lynn Lake (Canada), scheduled in July 1994.

The basic element of the GILDA telescope is a 6×6 cm^2 module composed by two Si detectors, each with a thickness of 380 μm, mounted back to back with perpendicular strips to give the X and Y coordinates (figure 1). In this experiment, two different strips widths are considered. For the 3.6 mm strips, each module contains 16 strips, while for the 125 μm ones it is possible to arrange 500 strips in each wafer (figure 2). The detectors are held in a special package which, when patched to form large surfaces, allows a minimal dead area for the sampling planes of the calorimeter. All the used materials are approved by NASA for space applications.

The principal constraints are imposed by the satellite in terms of volume, weight and available electric power. The free volume on the satellite is a cylinder 110 cm diameter and 70 cm in height, the available mass and electric power are respectively 700 kg and 350 W.

The baseline configuration of GILDA has a height of 40.8 cm, an area of 50×50 cm^2 and a total showering length of 10 X_0 (radiation lengths). A suitable arrangement of the electronics coupled to the calorimeter and of the anticoincidence system allows to match the 110 cm diameter of the available cylindrical volume. In the volume under the detector, the remaining digital electronics, interfaces and services can be located.

The stratigraphy of the instrument is shown in figure 3. The γ detector can be separated into two sections: the converter (or tracker) and the absorber. The first twenty planes form the converter zone, in which the silicon layers, made of 125 μm strips, are separated by tungsten plates of thickness 0.07 X_0. The distance between two contiguous planes is 1.0 cm. In each plane, 4000 silicon strips per view allow a very precise measurement of the direction of the incoming gamma ray. The granularity of the silicon and the thickness of the tungsten have been decided by detailed Monte Carlo studies and hardware developments and they represent the compromise between number of necessary electronic channels, distance between planes, power consumption (1.5 mW/ch), efficiency and angular resolution.

The last ten planes E_1...E_{10}, constituting the absorber, are composed of 3.6 mm silicon strips and separated by layers of active scintillating lead fibers, 1 X_0 total thickness. Between the converter and the absorber, an aluminum plate of 0.2 X_0 is placed in order to reduce the back scattering of particles from the bottom of the calorimeter. Each silicon plane is 1.6 cm far from the following.

The structure of the scintillating fibers is shown in figure 4. It has been built embedding polystyrene fibers emitting in the blue, 1 mm of diameter, between plastic deformations of lead foils 0.5 mm thick. Fibers are glued to the foils and run parallel to each other with a pitch of 1.35 mm. The overall structure has a fiber:lead:glue volume ratio of 48:42:10 and a sampling fraction of $\sim 14\%$ for a minimum ionizing particle; moreover, it has a density of ~ 5 g cm^{-3} and a X_0 of ~ 1.5 cm. This means that, in one radiation length, ten lead foils are interleaved with the same number of fibers. Prototypes have already been extensively tested [4],[5] with accelerator beams, showing that the lead scintillating fibers calorimeter has an energy resolution for γ of the order of $5\%/\sqrt{E(GeV)}$ for total containment. The solution of adopting these fibers is particularly attractive because HPK has developed compact PM's (PMT R5600 series) reduced to the same dimensions as a solid state detector and housed in a robust metal package 15 mm in diameter and 10 mm in length, while maintaining the same performances, high sensitivity and high speed as a conventional PM. The very low mass and the power consumption of the PMT R5600 (~ 100 mW) allow the use of the large number of PM needed for a fast trigger.

The configuration is completed with a plastic anticoincidence scintillator A_c (3 cm thick) around the converter zone of the calorimeter, and with two fibers scintillators (without the lead), one, E_{01}, after the first seven planes (that is after 0.49 X_0) and the other, E_{02}, after fourteen planes from the top of the detector. The introduction of the first one allows to obtain a threshold for gamma ray detection of 25 MeV.

2.1. Trigger

Two different triggers are adopted, for the low and high energy regions respectively:

- $\overline{A_c} \cdot (E_{01} \cdot OR \cdot E_{02})$, up to 1 GeV.
- for high energy, to avoid the same problems as EGRET, we do not use the anticoincidence scintillators. The trigger is constituted by the OR between E_{01} e E_{02}, with the request of having at least *two* of the following conditions for the energy deposited in the first five planes of the absorber:

  $E_2 > E_1$
  $E_3 > E_2$
  $E_4 > E_3$
  $E_5 > E_4$,

  to impose a shower behaviour for an entering particle. In this case, the elimination of crossing charged particles (like μ) and of particles inducing hadronic showers is realized on board with the aid of neural networks; several algorithms of pattern recognition, in fact, based on neural networks, have been developed by the WiZard collaboration with great success [6],[7].

3. Analysis method

For the simulation of gamma rays in the GILDA calorimeter we used the Geant 3.15 code. As a result of a number of optimizations, the energy threshold has been fixed at 10 keV; this means that GEANT follows a secondary particle until its energy is above or equal this value, then it drops it.

During the tests made at Cern with the prototype of the WiZard calorimeter, it has been possible to check the reliability of the Monte Carlo simulations, based on the Geant code, in reproducing real events. An excellent agreement between real and simulated data has been observed, as confirmed by figures 5 and 6. In figure 5 the total energy released in the calorimeter, obtained adding the signal of each silicon strip for both the views, as a function of the incoming gamma energy for both real data and Monte Carlo simulations, is showed, while in figure 6 the longitudinal development of a typical electromagnetic shower, induced by a 6 GeV electron, again for real and Monte Carlo events, is presented. The curve is obtained taking the value of the transversal energy deposit in each plane, for a sample of 2000 events, for the whole length of the prototype.

The calorimeter responses have been studied for gammas at energies of 20 MeV, 100 MeV, 500 MeV, 1 GeV, 10 GeV, 50 GeV, 90 GeV, with a statistical error of $\sim$ 2.2 %. Photons hit the calorimeter orthogonally, and in the center of the first plane.

Each layer of scintillating lead fiber has been simulated interleaving, for 10 times, 0.5 mm of lead with 1 mm of polystyrene, for a total of 1.5 cm of thickness ($\sim$ 1 X_0).

For each sensitive volume, a cut of 0.5 mip (minimum ionizing particle) on the energy released has been imposed, since our aim was to reproduce the experimental situation in which it is necessary to eliminate the noise of the electronics from the analysis; this implies that the following thresholds in energy are present:

- 70 KeV for each silicon strip (380 μm thick)
- 100 KeV for each layer of polystyrene (1 mm thick)
- 3 MeV for the anticoincidence plastic scintillator A_c (3 cm thick)

The γ energy is linearly related to the sum of the energies deposited in each lead scintillating fiber and in the X and Y silicon strips. The statistical fluctuations of this sum have been taken as an error and define the energy resolution of our apparatus.

To reconstruct the gamma incidence angle in our calorimeter, we developed an algorithm of track reconstruction, based on an iterative process. The track is identified with the axis of the shower. In fact, since the secondaries produced in an e.m. shower are more than 100 for gammas with energies greater than 1 GeV, their distribution is almost symmetric around the direction of the primary photon. The axis is determined by a linear iterative interpolation of the barycentres x_c of the transversal energy deposit of the shower in each plane:

$$x_c = \Delta \frac{\sum_i (i - 0.5) E_i}{\sum_i E_i}, \tag{1}$$

where Δ is the strip width and E_i is the energy deposited in the i-th strip (-0.5 because we simulated a beam hitting in the center of the silicon strip). The algorithm develops in the following steps:

1. it operates a linear fit of the barycentres of the transversal energy deposit in all the hit planes in the *absorber* (second half of the calorimeter), determining in this way a direction;
2. from this direction an area is extrapolated, with a fixed radius [1], for the *first three hit planes* of the tracker, and in this area it evaluates the barycentres. In this way, the process excludes the strips hit by back scattered particles;
3. with these three barycentres it determines a new direction, and the iterative process begins;
4. the track just evaluated will individuate an area in the following plane where it calculates a new barycentre;
5. with these four barycentres, the algorithm evaluates a new direction, and the process comes back to point 4.

The process stops when a direction converges, within a chosen error (10 mrad for us), with the previous one, or when the number of iterations overcomes the value of 20 (the number of planes in the tracker). To be significative, a trajectory must be determined by at least four points. Since in the first two planes of the detector the showering material (tungsten) is absent (see figure 3), we can use them as a secondary anticoincidence system for charged particles; in fact, if one of these two planes gives a signal, within one Moliere Radius, along the direction just determined, the particle is eliminated being recognized as charged. In conclusion, the gamma direction is given only by the tracker planes, where the granularity is very high, but the information of the absorber is preliminary used to eliminate from the fit tracks in the initial part of the detector due to back scattered secondaries. The reconstructed angles distribution, whose sigma furnishes the GILDA angular resolution, is dominated by multiple scattering up to energies of ~ 1 GeV and by the geometry of the Si planes at higher energies, and by the fluctuations in the shower developing.

4. Results

The energy resolution is shown in table 1 and in figure 7; its deterioration for high energies is related to the longitudinal leakage of the shower. For comparison, the relative contributions of the silicon detectors and the lead scintillating fibers are presented in tables 2 and 3 and in figure 7.

[1] We chose the Moliere Radius of our calorimeter (a radius in which 90% of the transversal development of the shower is contained), again evaluated by the simulations.

In conclusion, the total energy resolution of GILDA calorimeter is around $\sim 6\%$ / $\sqrt{E(GeV)}$, that is the combination of $\sim 18\%$ / $\sqrt{E(GeV)}$ of the silicon strips and $\sim 10\%$ / $\sqrt{E(GeV)}$ of the lead fibers, as far as the longitudinal leakage of the shower is negligible ($\leq$1 GeV). Finally in figure 8 a comparison between GILDA and EGRET energy resolutions is presented. Apart from very low energies (below 100 MeV), our telescope performances are better as compared with those of EGRET, even in the region where leakage is dominant.

In table 4 and in figure 9 the trigger efficiency and the total efficiency of GILDA are shown. The second one takes into account the loss of good events due to the track recognition algorithm previously described. It is easy to verify that the EGRET problems of efficiency for high energy gamma rays have been overcome.

The results of the angular resolution are plotted in figure 10 together with the EGRET ones. Our pointing capacity comes out to be better than that of EGRET in all the energetic spectrum considered.

The GILDA absorber can also measure the direction of the gamma that escapes materialization in the tracker with a larger solid angle and full efficiency; for these photons the angle is measured by reconstructing the shower direction in the absorber.

Finally, in table 5 we report some geometrical characteristics of our calorimeter, compared with EGRET.

5. Conclusions

Our simulations have shown that the GILDA instrument is able to reach significatively better performances than the experiment EGRET on the CGRO, though having less area and weight; the main characteristics that make this telescope more efficient are:

- the use of silicon strips instead of spark chambers as main device for reconstructing the gamma's trajectory; in this way, we avoid the problem of gas refilling, high voltages and dead time (silicon strips have lower dead time than gas detectors). Moreover, we can reach a resolution of the order of a hundred of microns, instead of few millimeters;
- the elimination of the anticoincidence counters for the high energy trigger, so that an efficiency of 70% up to 100 GeV can be reached.
- the constitution of a whole calorimeter with 10 X_0, formed by scintillating lead fibers, instead of the 8 X_0's of the EGRET instrument;
- the elimination of TOF, with the consequential increase of the acceptance and decrease of the energetic detection threshold (25 MeV for GILDA and 35 for EGRET); again, the pattern recognition algorithms will substitute, off line, the TOF system, recognizing an upward going particle from a downward.

An important point is that the modularity of our calorimeter consents to easily change his lateral dimensions (at least in the range 6 cm $\div$ 200 cm) to tune the area, in an advanced project phase, to the maximum value permitted by the total weight of the payload. Of course, the collected statistics increases widening the area.

REFERENCES

1. Kanback G. et al., *Space Science Rev.*, **49**, 69, (1988).
2. Golden, R. L. et al., *Il Nuovo Cimento*, **105 B, 2**, 191, (1990).
3. Bocciolini M. et al., *NIM*, **A333**, 560, (1993).
4. Hertzog D. W. et al., *NIM*, **A294**, 446, (1990).
5. Bianco S. et al., *NIM*, **A315**, 322, (1992).
6. M.Candusso, M. Casolino, M. P. De Pascale, A. Morselli, P. Picozza, R. Sparvoli, " Stochastic Preprocessing to a Neural Network in High Energy Physics Particle Recognition", Physics Comp. '94, Lugano (CH), 22-26/8/94.
7. M.Candusso, M. Casolino, M. P. De Pascale, A. Morselli, P. Picozza, R. Sparvoli, " Neural Network with Stochastic Preprocessing for Particle Recognition in Cosmic Ray experiments", proceedings of "Frontier Detectors for Frontier Physics", 6th Pisa meeting on advanced detectors, Isola d'Elba, Italy, 22-28/5/94, in press (NIM proceedings series).

Energy (MeV)	E deposited (MeV)	σ(E) (MeV)	Resolution (%)
100	18.70	3.28	17.5
500	101.4	7.41	7.3
1000	200.0	13.69	6.8
10000	1715.2	144.3	8.4
50000	7123.1	924.4	13.0

Table 1: *Total energy resolution for GILDA telescope.*

Energy (MeV)	E dep. in Si-D (MeV)	σ(E) (MeV)	Resolution (%)
100	4.68	2.14	45.8
500	12.17	3.66	30.0
1000	20.47	4.75	23.2
10000	149.1	19.13	12.8
50000	603.0	88.60	14.7

Table 2: *Silicon detectors energy resolution.*

Energy (MeV)	E dep. in fibers (MeV)	σ(E) (MeV)	Resolution (%)
100	13.54	4.21	31.1
500	88.36	8.84	10.0
1000	180.0	17.29	9.6
10000	1565.0	132.3	8.5
50000	6476.1	877.2	13.5

Table 3: *Fibers detectors energy resolution.*

Energy (MeV)	Trigger efficiency(%)	Trigger + analysis efficiency(%)
100	48.9	14.6
500	57.1	31.6
1000	55.9	48.5
10000	68.3	65.6
50000	78.4	77.1

Table 4: *Efficiency for GILDA telescope; the first column presents the trigger efficiency only, while the second considers the trigger plus the analysis.*

Characteristics	EGRET	GILDA
Effective area	0.16 m^2	0.14 m^2 (500 MeV)
(area $\times$ efficiency)	0.12 m^2	0.13 m^2 (1 GeV)
	0.07 m^2	0.17 m^2 (10 GeV)
Solid angle	0.6 sr	0.92 sr
Point source	5.4×10^{-8}	6.45×10^{-9} (0.1 GeV)
sensitivity	1.2×10^{-8}	7.23×10^{-10} (1 GeV)
(ph cm^{-2} s^{-1})	2.1×10^{-8}	3.60×10^{-10} (10 GeV)
Volume	4.8 m^3	0.102 m^3
Mass	1830 kg	700 kg
Power	190 W	250 W

Table 5: *Some of the principal characteristics of GILDA telescope compared with those of EGRET.*

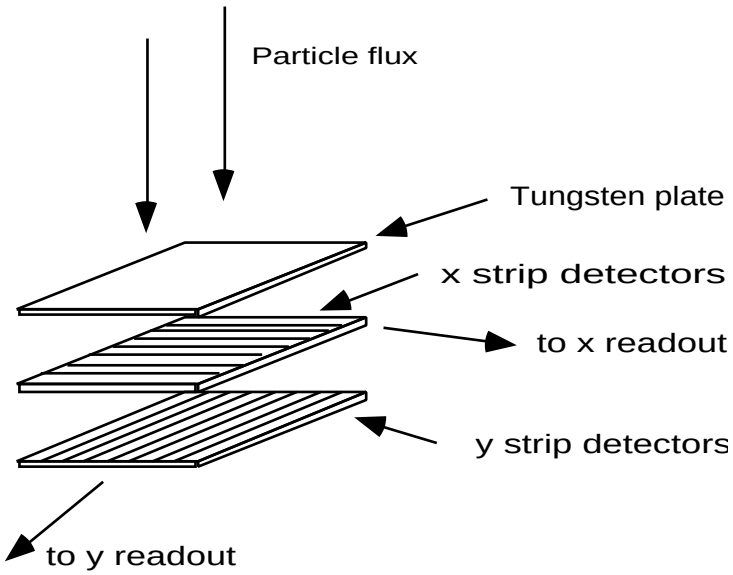

Figure 1. *The silicon wafer, main element of the WiZard calorimeter.*

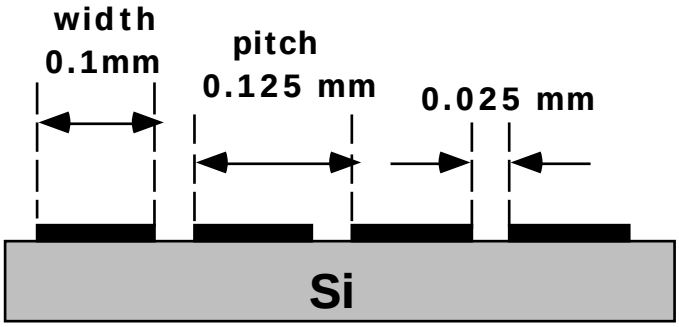

Figure 2. *The 125 micron silicon strips.*

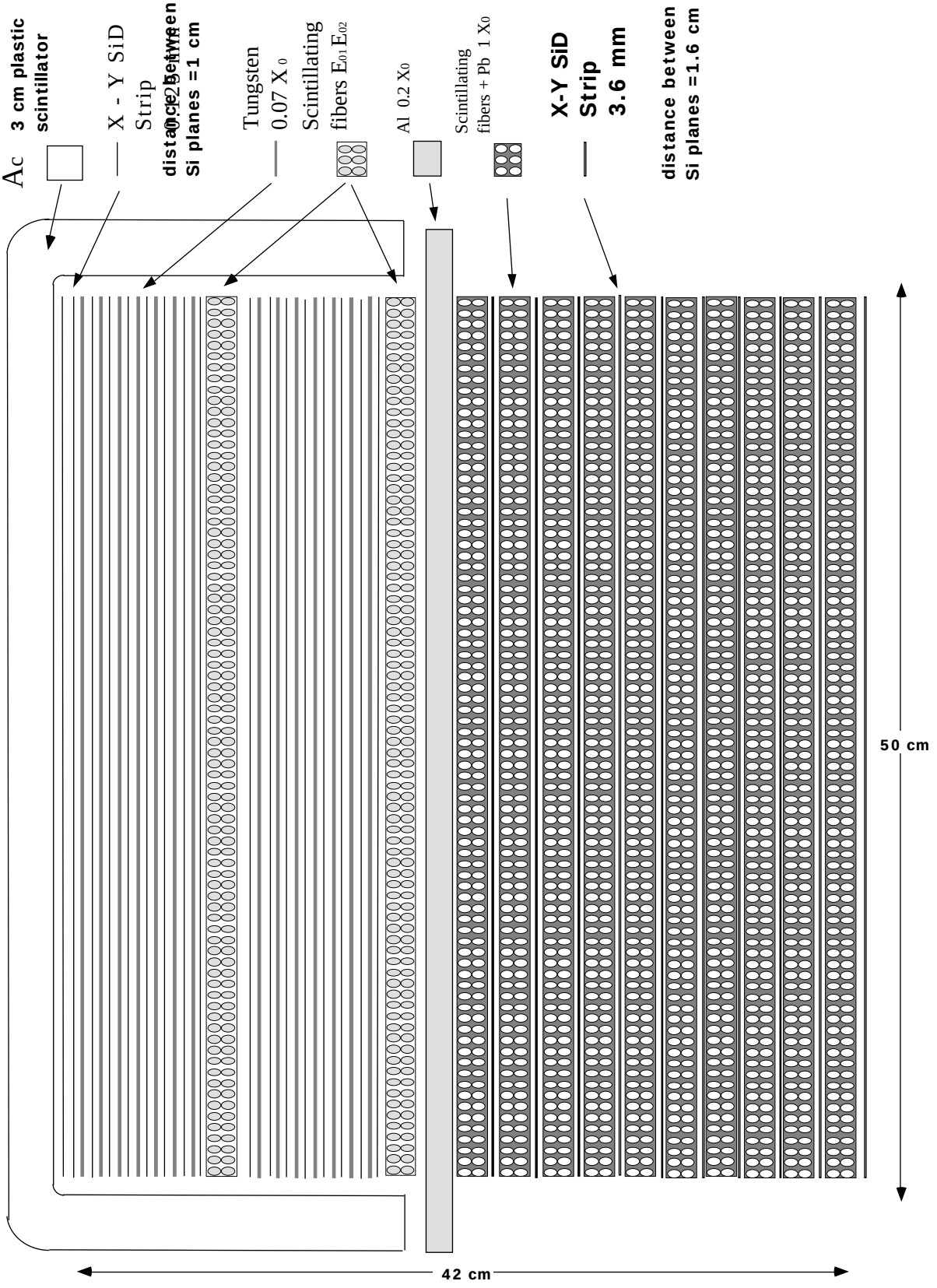

Figure 3. *The stratigraphy of the GILDA detector.*

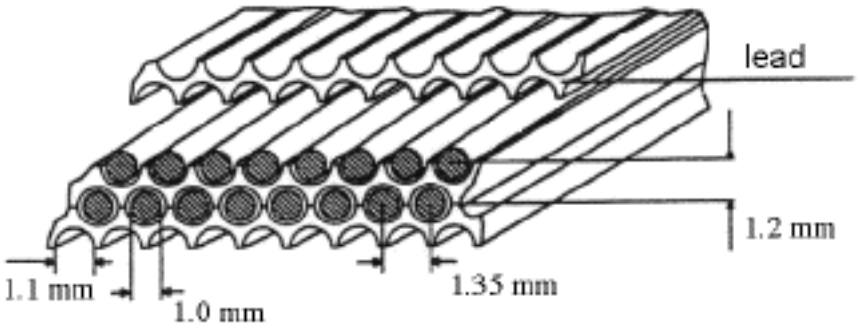

Figure 4. *Structure of the lead scintillating fibers.*

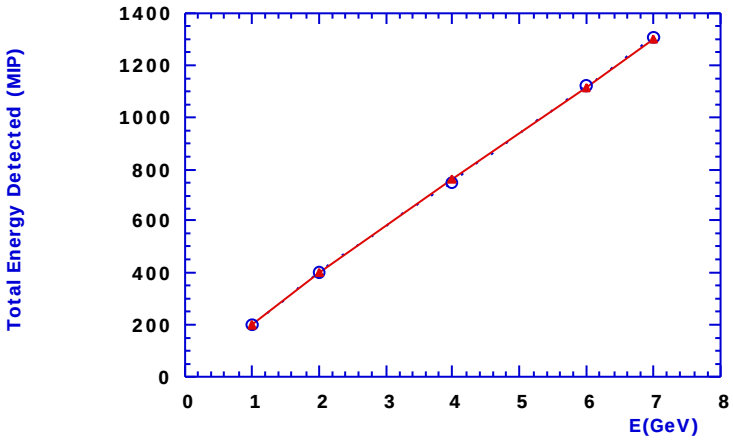

Figure 5. *Energy linearity of the prototype of the WiZard calorimeter; real data (triangles), MC data (bullets).*

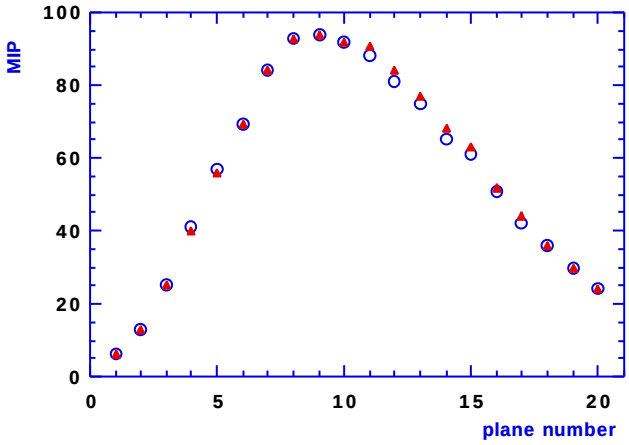

Figure 6. *Longitudinal development of an electromagnetic shower for the prototype of the WiZard calorimeter; real data (triangles), MC data (bullets).*

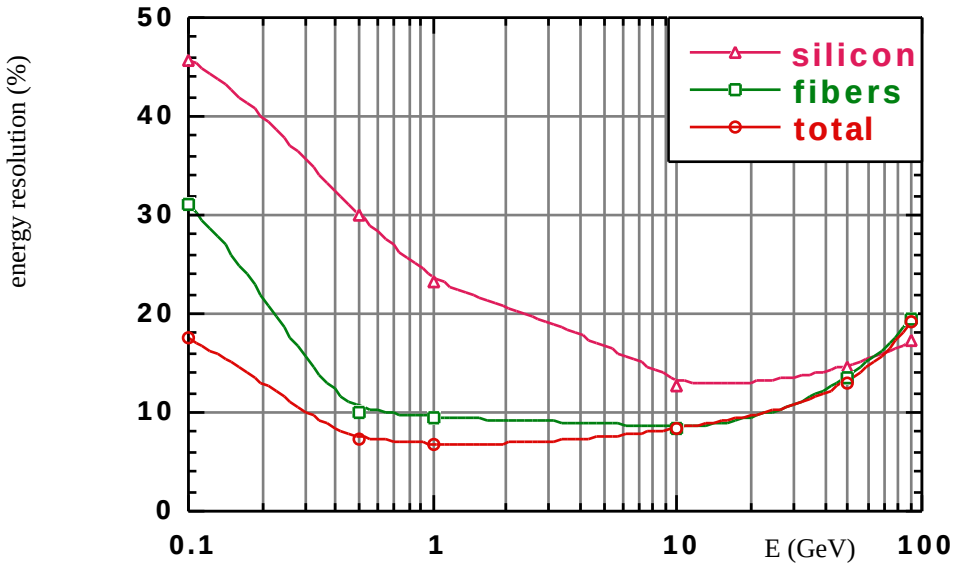

Figure 7. *Simulated behaviour of GILDA energy resolution as a function of energy for lead fibers (squares), silicon strips (triangles) and total (sum of the two: bullets).*

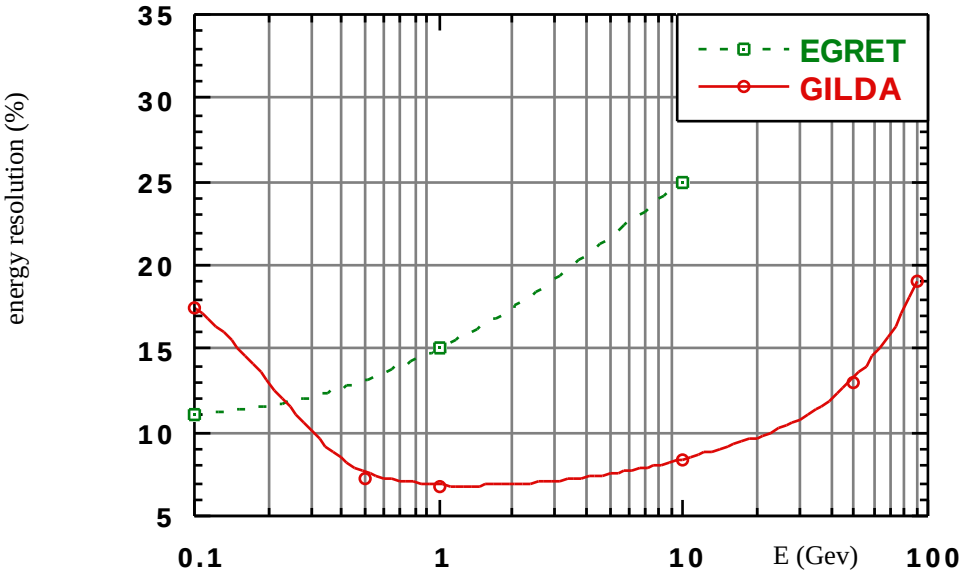

Figure 8. *Simulated GILDA energy resolution, compared with EGRET.*

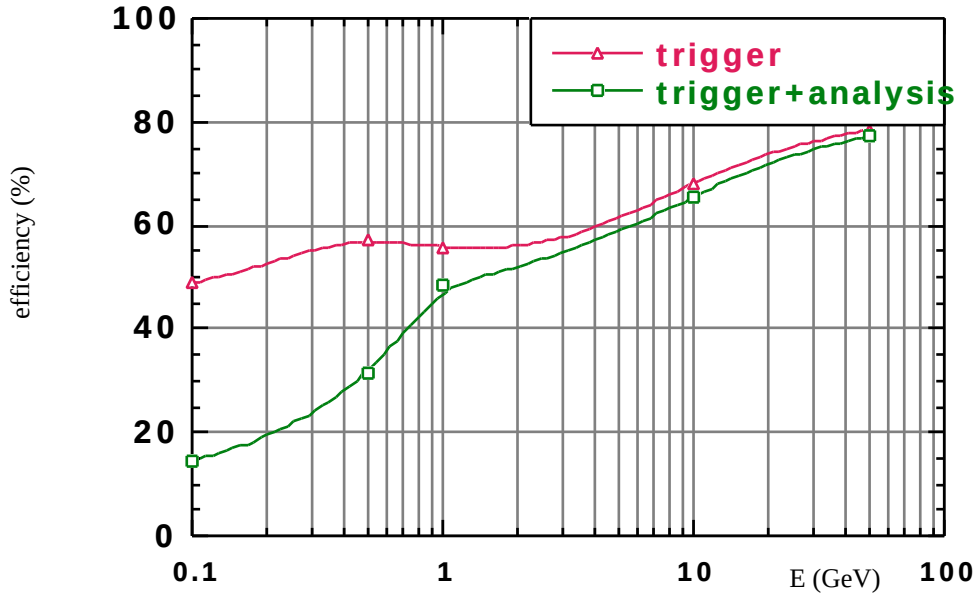

Figure 9. *GILDA efficiency, before and after the analysis.*

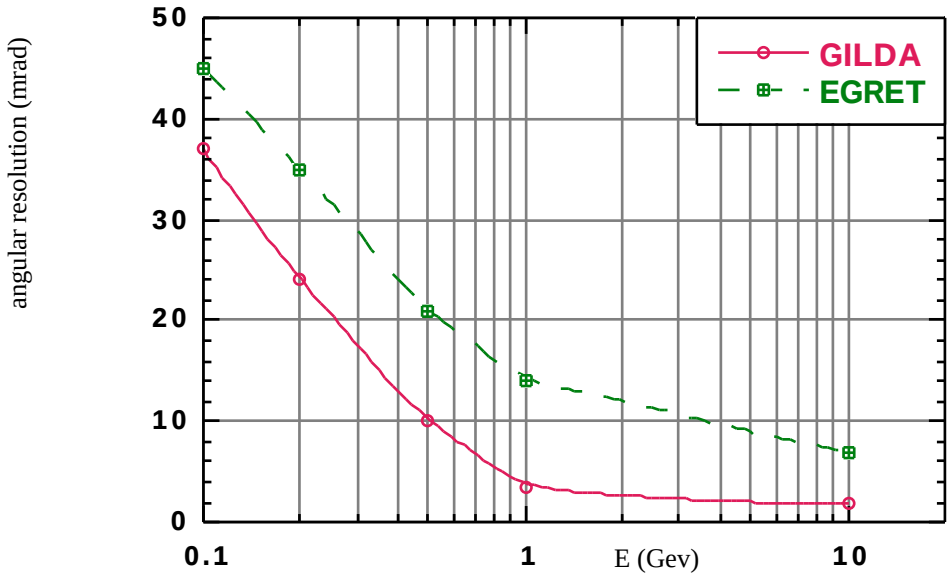

Figure 10. *Simulated GILDA angular resolution, compared with EGRET.*